AD-A133 311 CHEMISTRY RESEARCH OF OPTICAL FIBERS(U) SACHS/FREEMAN ASSOCIATES INC BOWIE MD R J GINTHER ET AL. 27 SEP 82 SFA82-002 SBI-AD-E001 403 N00173-80-C-0232 1/1

UNCLASSIFIED F/G 20/6 NL

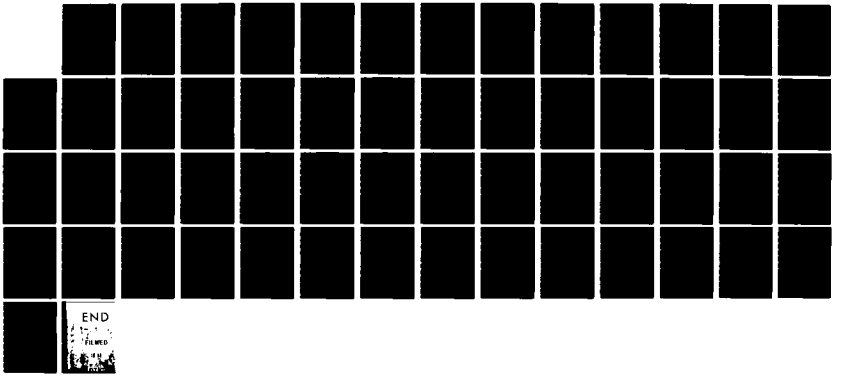

END

FILMED

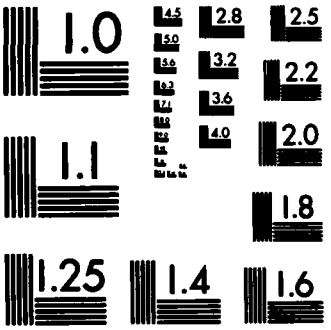

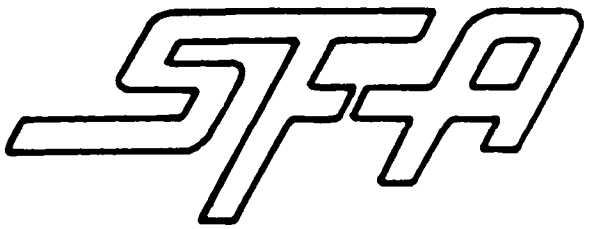

Security Classification: Unclassified

SFA82-002

CHEMISTRY RESEARCH OF OPTICAL FIBERS

R. J. Ginther, K. H. Levin, PhD
Sachs/Freeman Associates, Inc.
14300 Gallant Fox Lane
Suite 214
Bowie, MD 20715

27 September 1982

Final Report for Period 23 June 1980 - 1 September 1982

Prepared for

NAVAL RESEARCH LABORATORY
Optical Sciences Division, Code 6570
4555 Overlook Ave., S.W.
Washington, DC 20375

SACHS/FREEMAN ASSOCIATES, INC.

14300 GALLANT FOX LANE, SUITE 214, BOWIE, MARYLAND 20715 301-262-4400

SECURITY CLASSIFICATION OF THIS PAGE (When Data Entered)

REPORT DOCUMENTATION PAGE

READ INSTRUCTIONS BEFORE COMPLETING FORM

1. REPORT NUMBER: SFA-RD-80-C-0232 ; BP0205	2. GOVT ACCESSION NO.: AD-A133 311
3. RECIPIENT'S CATALOG NUMBER:	
4. TITLE (and Subtitle): CHEMISTRY RESEARCH OF OPTICAL FIBERS	5. TYPE OF REPORT & PERIOD COVERED: 23 June 1980 - 1 Sep 1982 Final Report
	6. PERFORMING ORG. REPORT NUMBER: SFA-82-002
7. AUTHOR(s): R. J. Ginther, K. H. Levin, PhD (g.H. Sigel, D.C. Tran)	8. CONTRACT OR GRANT NUMBER(s): N00173-80-C-0232
9. PERFORMING ORGANIZATION NAME AND ADDRESS: Sachs/Freeman Associates, Inc., 14300 Gallant Fox Lane, Suite 214, Bowie, Maryland 20715	10. PROGRAM ELEMENT, PROJECT, TASK AREA & WORK UNIT NUMBERS:
11. CONTROLLING OFFICE NAME AND ADDRESS: Naval Research Laboratory, Optical Sciences Div., Code 6570, 4555 Overlook Ave., SW, Washington, DC 20375	12. REPORT DATE: 9/27/82
	13. NUMBER OF PAGES:
14. MONITORING AGENCY NAME & ADDRESS(if different from Controlling Office): DCASMA, Baltimore, Rm. 200, 300 E. Joppa Road, Towson, MD 21204	15. SECURITY CLASS. (of this report): Unclassified
	15a. DECLASSIFICATION/DOWNGRADING SCHEDULE:

16. DISTRIBUTION STATEMENT (of this Report)

Approved for Public Release; Distribution Unlimited

17.

18.

19. KEY WORDS (Continue on reverse side if necessary and identify by block number)

Optical fibers materials, preparation, materials, characterization

20. ABSTRACT (Continue on reverse side if necessary and identify by block number)

The Optical Techniques Branch of the Optical Sciences Division requires understanding of their mission and related problems in the areas of fiber and integrated optics directed towards using light guiding optical components in high capacity data transfer systems. Experimental and theoretical research covered in this report includes: preparation of optical fibers, and fiber optic materials, purification and synthesis of starting materials and the characterization of the optical fibers.

DD FORM 1 JAN 73 1473 EDITION OF 1 NOV 65 IS OBSOLETE

Unclassified

SECURITY CLASSIFICATION OF THIS PAGE (When Data Entered)

FINAL REPORT

for

CONTRACT NO. N00173-80-C-0232

1.0 INTRODUCTION

This is a final report for research provided to the Optical Techniques Branch, Code 6570 at NRL. It explains briefly the areas and the nature of the research provided. Attached papers give details of the research that has taken place under this contract. Major accomplishment to aid this research was the design and fabrication of optical drawers, design and installation of an optical absorption test stand, a chemical vapor deposition laboratory, and materials preparation.

2.0 MATERIALS PREPARATION

Advancements have been concerned with the preparation of fluoride glasses for ultra low loss fibers. Composition for cone and cladding glasses have been further enhanced to provide increased resistance to devitrification in synthesis and subsequent processing. Reproducible procedures for the preparation of pure fluorides of girconium, barium, lithium, aluminum, lanthanum, and lead were obtained.

Additional work was concerned with further removal of oxygen from these materials and the simplification of some of the extended procedures now being employed.

3.0 FIBER PREPARATION

An optical fiber drawing laboratory for the silica based glass has been set up. This included the design and fabrication of a draw tower (Figure 1), installation of a Lepel induction furnace as a heat source and integration of a closed loop feedback control system.

An infrared fiber drawing apparatus has been designed and fabricated (Figure 2). Interfacing was not completed at the termination of the contract performance period.

Design of a modified chemical vapor deposition (MCVD) system was completed. All major components were at NRL awaiting assembly and integration.

4.0 CHARACTERIZATION OF GLASSES AND FIBERS

A laboratory has been established dedicated to the measurement and characterization of the optical properties of bulk and fiber samples of glass, especially the new infrared transmitting glass being developed at NRL. These properties include the total loss of the fibers, absorption and scattering loss

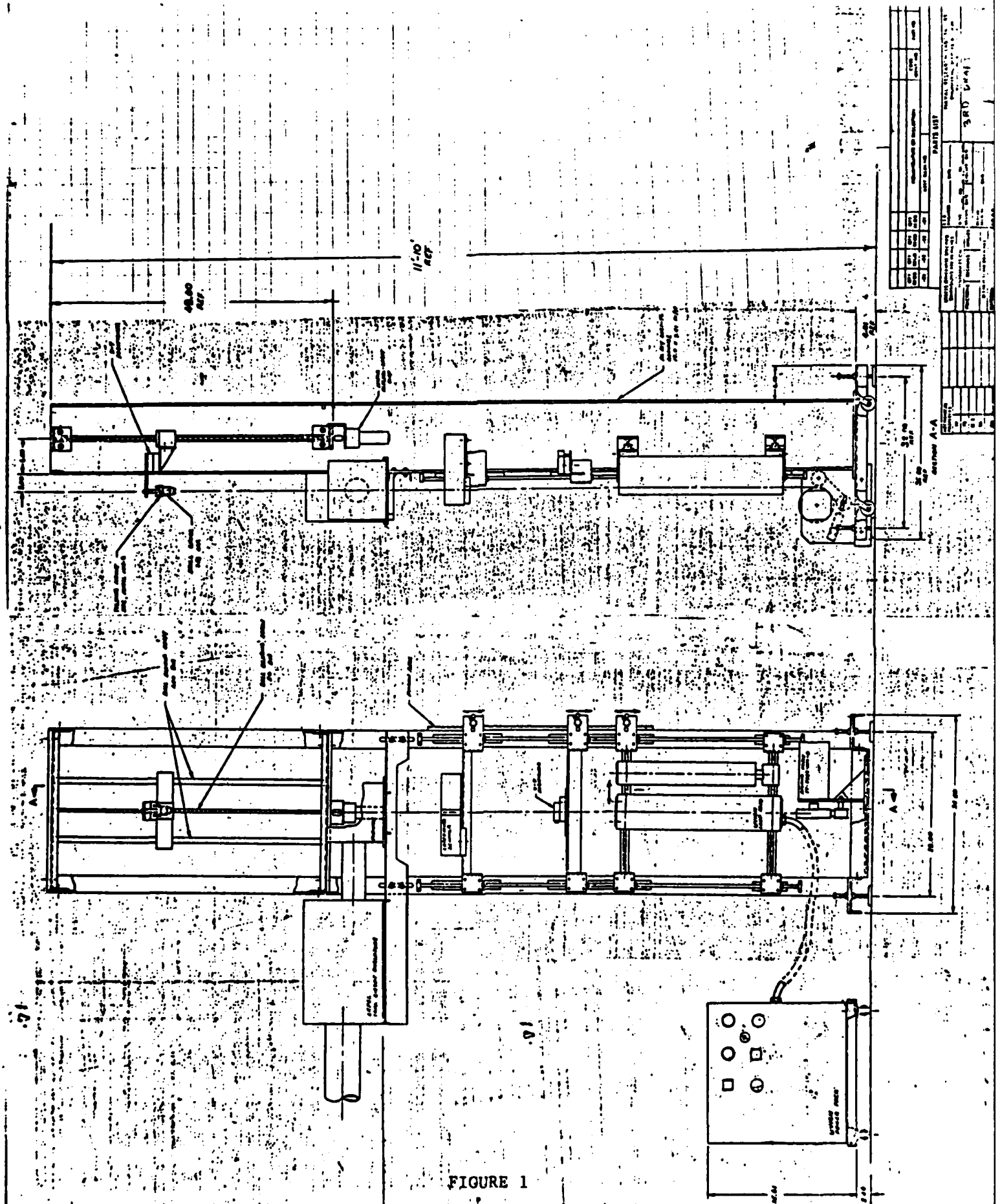

FIGURE 1

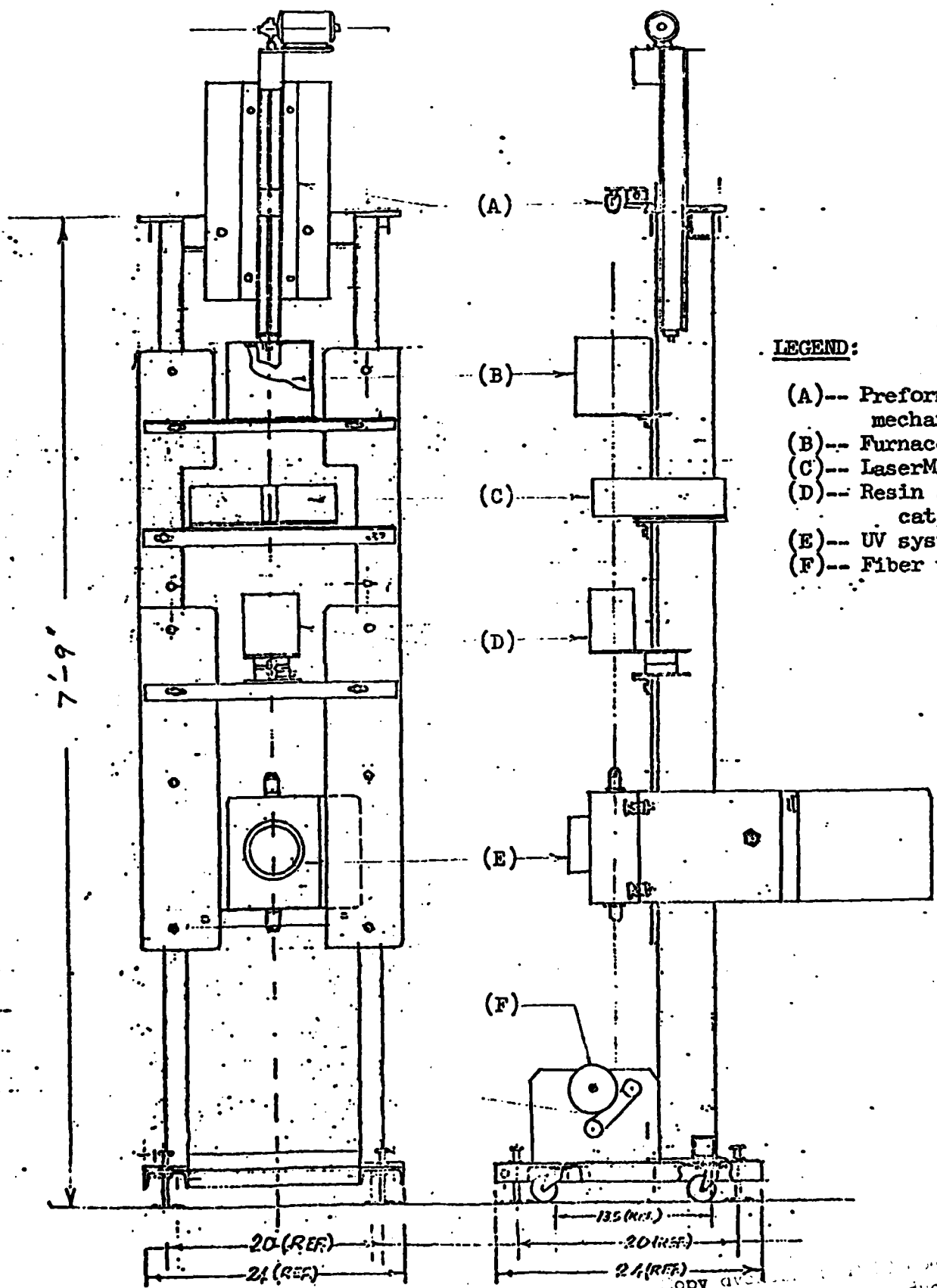

FIGURE 2: INFRARED FIBER DRAWING APPARATUS

NAVAL RESEARCH LABORATORY
WASHINGTON, D.C. 20375

of bulk and fiber samples, refractive index, fiber numerical aperture, and radiation hardness. In support of these objectives, the laboratory contains a number of new pieces of equipment. A diagram of the laboratory is shown in Figure 3. In air-floatation optical table supports the experiments. A separate table containes the computer, printer, and plotter, as well as a lock-in amplifier. A cabinet contains many optical components and other equipment. The room also contains a new state-of-the-art infrared spectrophotometer. Lasers in use include a large Nd:Yag, argon-ion, and HeNe.

A new experimental test stand has been designed and installed to measure the total loss of optical fibers, especially in the infrared region of the spectrum. The system consists of a very intense infrared source (a Nernst glower), and a very sensitive cooled detector. A block diagram of the apparatus is shown in Figure 4. The system is being routinely used to characterize glass fibers. In addition, the scattering loss of the fibers is measured with a test system consisting of an integrating sphere detector and an argon-ion laser.

The infrared absorption of bulk samples of glass has been measured using laser calorimetry. The spectral range spans the visible through infrared using several types of lasers. This technique has been extended to glass fibers by using an interferometric method to detect thermal expansion of the fiber. A diagram of this system is shown in Figure 5.

In addition to the above, a study has been completed on the Raman spectra of irradiated glass. This study has been useful in determining the damage effect of the radiation on the glass.

5.0 SCIENTIFIC DOCUMENTATION

Reprints of technical publications that have resulted from this work begin on page 8. These papers give details of the research that has taken place under this contract.

LABORATORY FOR OPTICAL MEASUREMENTS

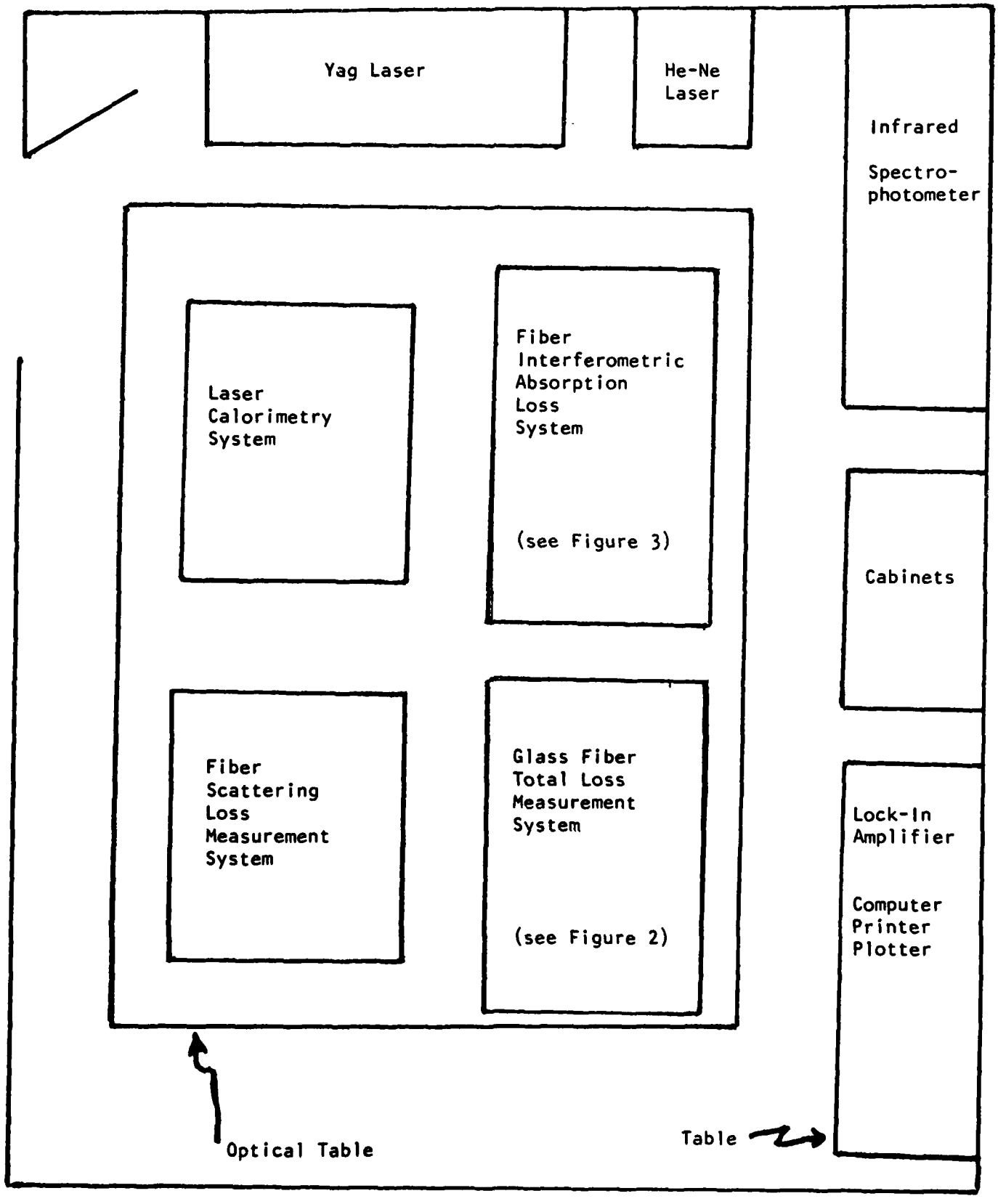

FIGURE 3

IR FIBER SPECTRAL LOSS MEASUREMENT SYSTEM

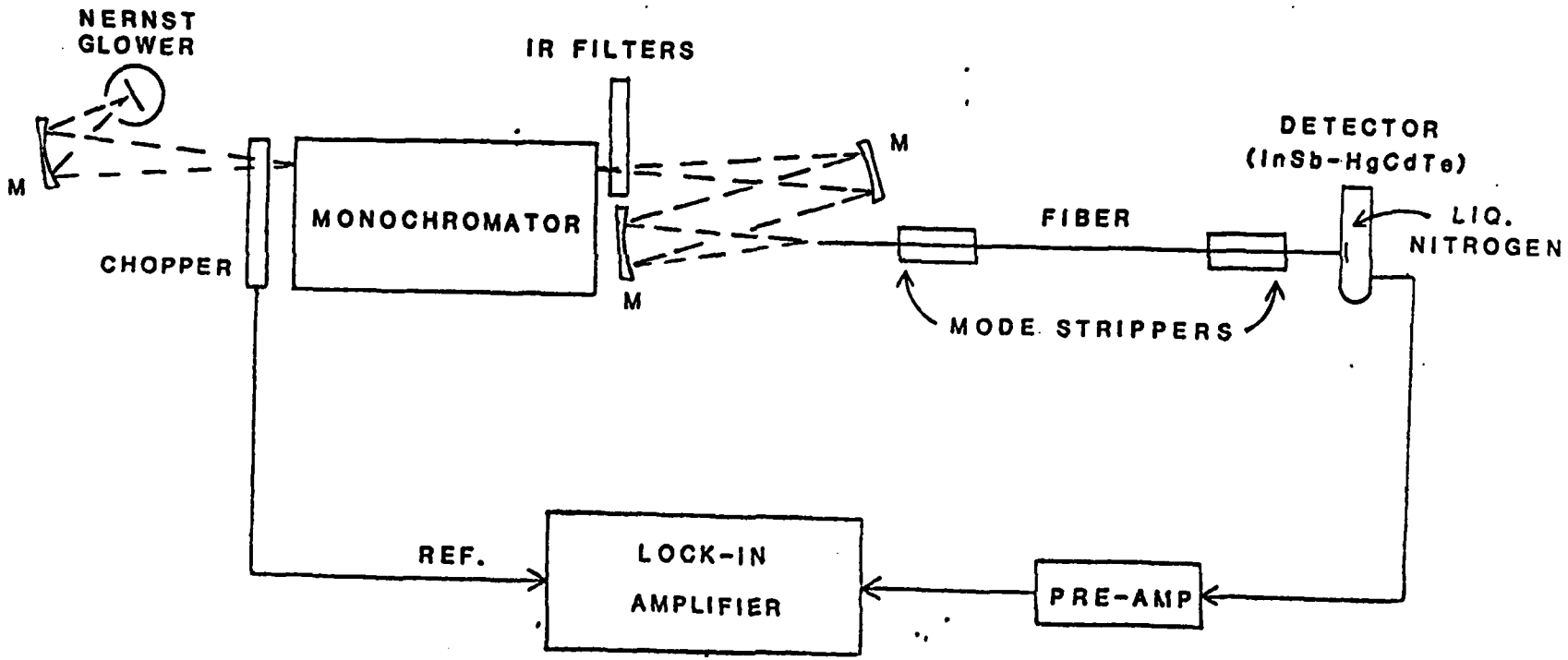

FIGURE 4

LASER INTERFEROMETRIC FIBER ABSORPTION MEASUREMENT

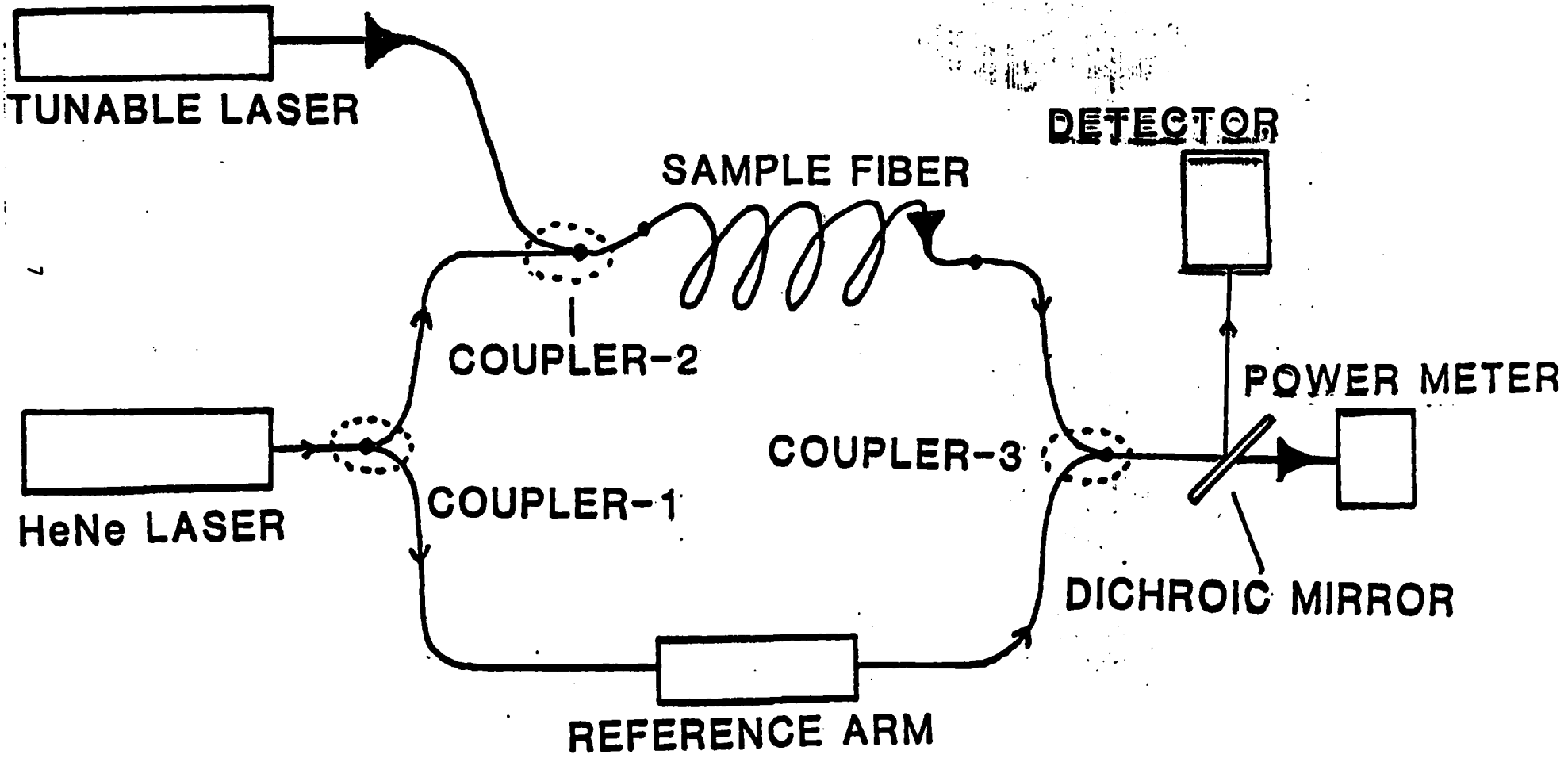

FIGURE 5

SOCIETY OF GLASS TECHNOLOGY

First international symposium on halide and other nonoxide glasses

Churchill College, Cambridge

23-26 March 1982

Extended abstracts received by 26 February 1982

OPTICAL PROPERTIES OF FIBER AND BULK FLUOROZIRCONATE GLASSES

K. H. Levin*, D. C. Tran, R. J. Ginther, G. H. Sigel, Jr., and K. H. Fiedler**
Naval Research Laboratory
Washington, DC 20375

There has recently been much interest shown in fluorozirconate glasses due to their wide optical transmission range, and possibly very low loss in the mid-infrared region of the spectrum. In addition, these glasses can be pulled into fibers of extended lengths. We have measured the optical properties of samples of both bulk and fiber fluorozirconate glass in the ZrF_4 - BaF_2 - LaF_3 - AlF_3 - LiF system. These properties include the absorption in bulk samples, fiber total loss spectra, fiber scattering loss, radiation effects, and Raman spectra.

The absorption of bulk samples in the transparent region was determined using laser calorimetry. At .63 microns, the absorption was found to be 1400 dB/km, probably due to transition metal impurities. The absorption at 3.4 microns was 1600 dB/km, due to water impurity.

Fibers were pulled from the bulk glass having a diameter of about 100 microns and a length of several hundred meters. The total loss of the fibers was measured with the experimental set-up shown in Figure 1. Chopped infrared radiation from a Nernst glower passed through a monochromator and order blocking filters. The radiation was focused onto the fiber with concave mirrors having an N.A. of .1. The radiation from the output end of the fiber was detected with a cooled InSb detector, and the signal passed through a low-noise preamp and into a lock-in amplifier. The cut-back method was used to determine the fiber loss. The loss spectrum for a typical fiber is shown in Figure 2. The water peak at 2.8 microns is evident. The scattering component of the total loss was measured using an integrating sphere. These results, as well as the absorption data from laser calorimetry on bulk samples, are also shown in Figure 2.

To determine the effect of ionizing radiation on the glass, bulk samples were irradiated at a dose of 10^7 rads (Si) by a ^{60}Co source. The irradiated samples had a light tan color, although no change in their infrared transmission was seen. The u.v., visible, and infrared transmission spectra of the irradiated samples are shown in Figures 3 and 4. The u.v. edge can be seen to shift towards longer wavelengths with increasing dosage. Laser calorimetry at 3.4 microns indicated no change in the infrared absorption for the irradiated sample. The Raman spectrum of the irradiated sample is shown in Figures 5 and 6. The main peak at 579 cm^{-1}, due to ZrF_4 stretching vibrations, is unchanged by the irradiation. However, the low frequency modes are intensified, probably due to some structural damage occurring in the glass network.

* Sachs/Freeman Associates, Inc.
Bowie, MD 20715

**Georgetown University
Washington, DC 20057

FIFTH TOPICAL MEETING
ON
OPTICAL FIBER COMMUNICATION
13–15 APRIL 1982
OSA/IEEE
PHOENIX, ARIZONA

Digest of Technical Papers

PREPARATION AND CHARACTERIZATION OF ZIRCONIUM FLUORIDE BASED GLASS FIBERS

D. C. Tran, R. J. Ginther, G. H. Sigel, Jr., and K. H. Levin
Naval Research Laboratory
Code 6570
Washington, DC 20375
(202)767-3487

ABSTRACT

Optical fibers in lengths approaching 1 km have been prepared for the first time from a ZrF_4-BaF_2-LaF_3-AlF_3-LiF-PbF_2 glass system having improved viscosity-temperature characteristics. Fiber drawing techniques and experimental optical attenuation data are reported.

This paper would not be appropriate for a poster session.

PREPARATION AND CHARACTERIZATION OF ZIRCONIUM FLUORIDE BASED GLASS FIBERS

D. C. Tran, R. J. Ginther, G. H. Sigel, Jr., and K. H. Levin
Naval Research Laboratory
Code 6570
Washington, DC 20375
(202)767-3487

Among all infrared transmitting materials, ZrF_4 based-glasses seem very promising for the preparation of ultra low loss fiber waveguides since they exhibit a potential loss as low as 10^{-2} dB/km at 4.4 μm, and appear to possess adequate mechanical properties, chemical stability and environmental resistance.[1,2] For long distance, repeaterless data links for communications, it is essential that these glasses can be drawn into fibers of extended lengths.

Earlier attempts on fiber draw using a 57.5 ZrF_4-33.5 BaF_2-5.5 LaF_3-3.5 AlF_3 glass composition often resulted in devitrification which is largely due to a narrow working range and a steep viscosity-temperature profile. This paper will discuss compositional modifications which have been successful in developing glasses which exhibit excellent fiber drawing characteristics. As shown in Fig. 1, the addition of LiF to the above system still results in a high activation energy for viscous flow of about 171 kcal/mole although the glass transition temperature is substantially lowered. The addition of PbF_2 on the other hand, gives rise to a sharp drop in activation energy to 88 kcal thus decreasing significantly the slope of the viscosity-temperature profile. The presence of PbF_2 further extends the glass working range by lowering the glass softening point from ~ 300°C to ~ 283°C. Using the PbF2 doped glass, high quality fibers of extended lengths reaching 1 km have been drawn for the first time. X-ray diffraction methods reveal no evidence of crystallization in fibers

so prepared. The improved viscosity-temperature characteristics of the newly developed glass compositions have made it possible to employ a crucible drawing technique rather than the preform approach which is less attractive for continuous fiber drawing. The fiber drawing apparatus is illustrated in Fig. 2. It consists of a specially designed Engelhard® platinum crucible with a tapered down bottom; the crucible is contained inside a fused silica tube which is placed in an enclosed furnace; the furnace is continuously purged with dry Argon. Cullets of glass are charged into the crucible and are preheated at 150°C prior to being drawn into fibers at around the softening point. Absorption and scattering data for both the bulk glass and optical fibers will be presented and interpreted. This will include both laser calorimetric and spectrophotometric results.

References

1. J. R. Gannon, Frontiers of Glass Science, LA, July 16-18, 1980.
2. R. J. Ginther and D. C. Tran, Technical Digest, 3rd International Conference on Integrated Optics and Optical Fiber Communication, April 27-29, 1981.

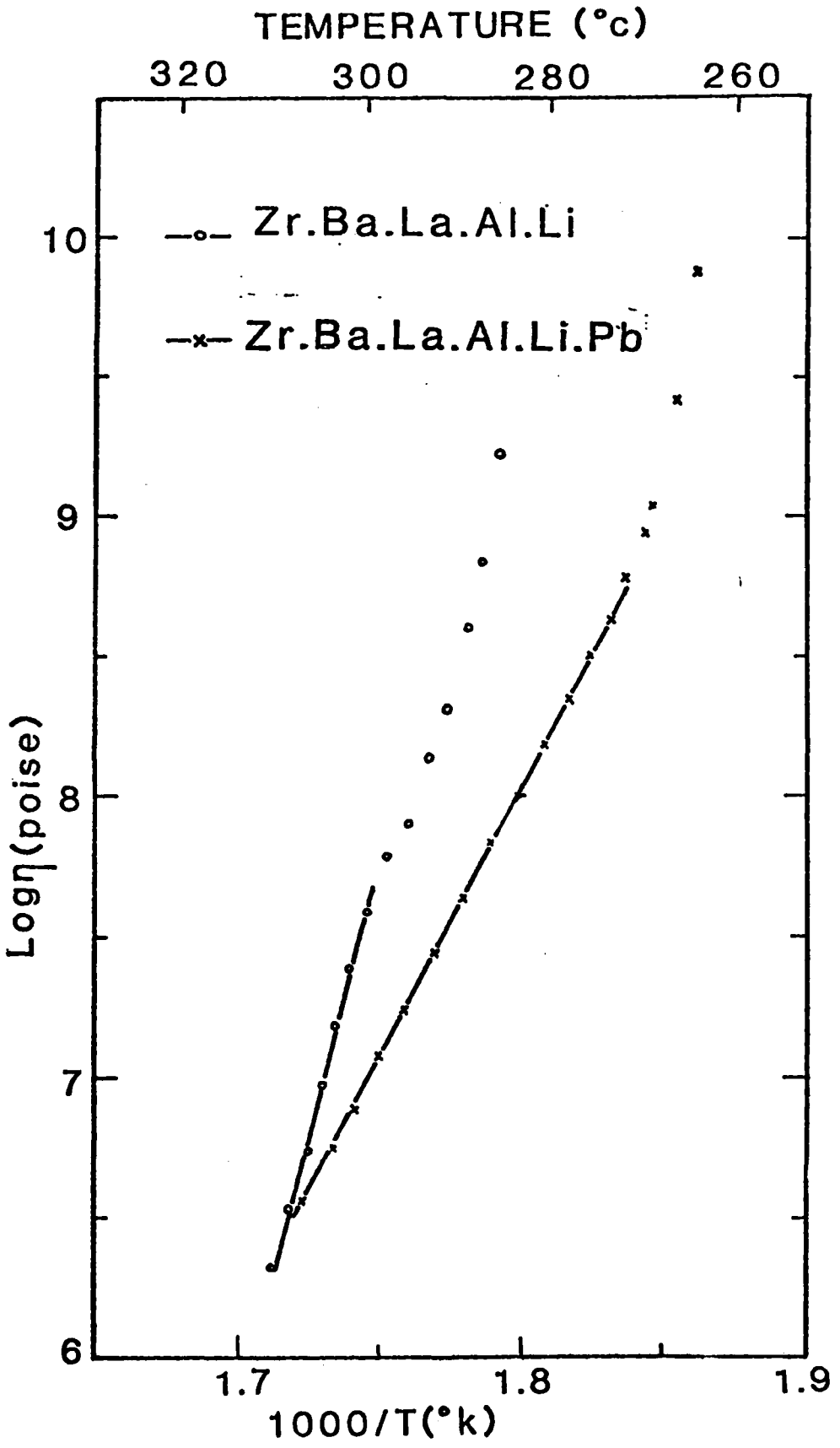
TEMPERATURE (°c)
320
300
280
260
Zr.Ba.La.Al.Li
Zr.Ba.La.Al.Li.Pb
10
9
8
7
6
Logη(poise)
1.7
1.8
1.9
1000/T(°k)

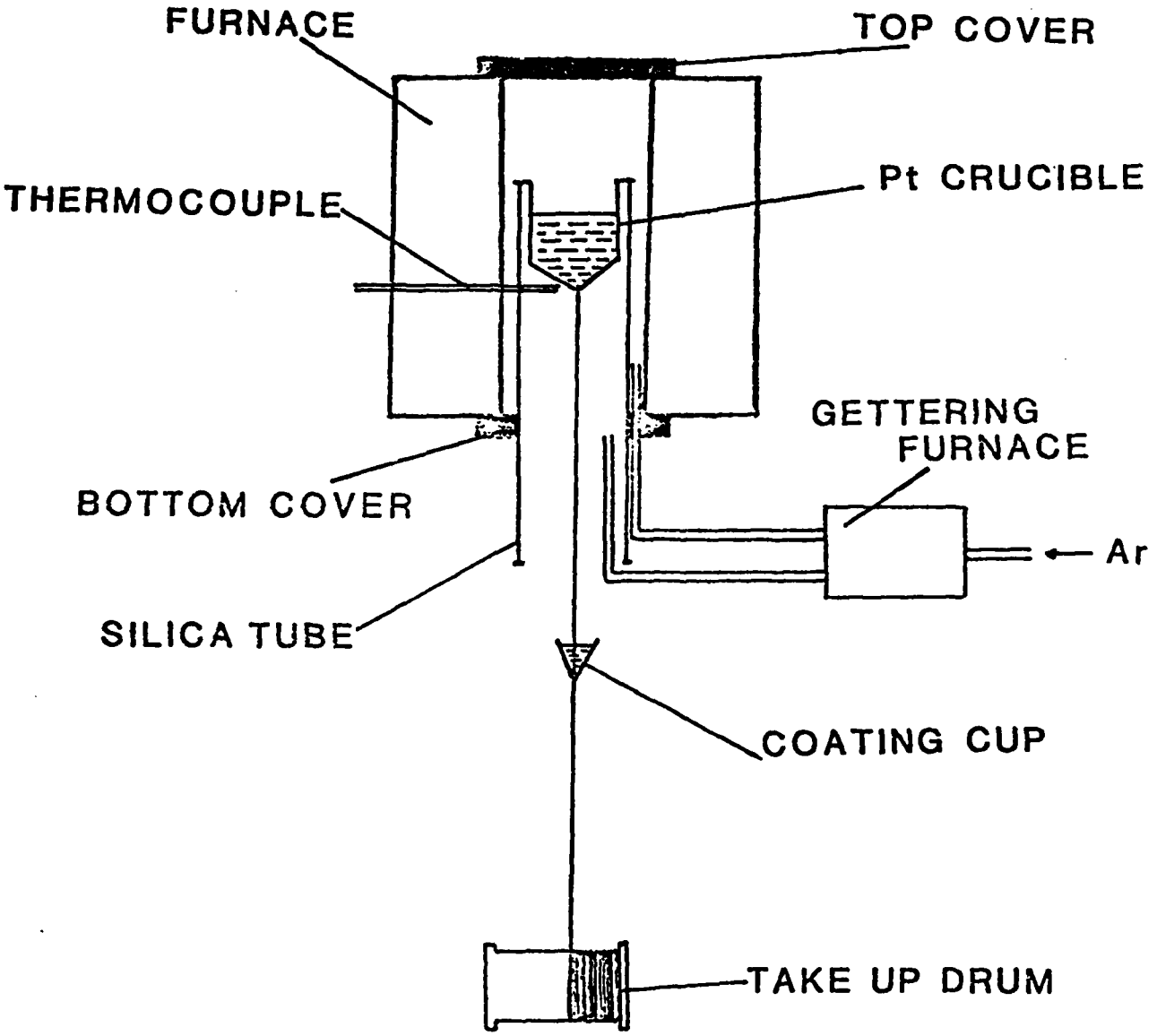
FURNACE
TOP COVER
THERMOCOUPLE
Pt CRUCIBLE
GETTERING
FURNACE
BOTTOM COVER
Ar
SILICA TUBE
COATING CUP
TAKE UP DRUM

To be published in "Glass Technology"

OPTICAL PROPERTIES OF FIBER AND BULK ZIRCONIUM FLUORIDE GLASS

K. H. Levin,* D. C. Tran, R. J. Ginther and G. H. Sigel, Jr.
Naval Research Laboratory
Washington, DC 20375

ABSTRACT

The optical properties of bulk samples as well as cladded and uncladded fibers of zirconium fluoride based glass have been measured. The loss mechanisms of the fibers are compared to those of the bulk glass. In particular, the scattering loss of our bulk samples was found to be very low, and followed a λ^{-4} wavelength dependence.

*Sachs Freeman Associates, Inc.
Bowie, MD 20715

OPTICAL PROPERTIES OF FIBER AND BULK ZIRCONIUM FLUORIDE GLASS

K. H. Levin, D. C. Tran, R. J. Ginther and G. H. Sigel, Jr.
Naval Research Laboratory
Washington, DC 20375

There has recently been much interest shown in zirconium fluoride based glasses due to their wide optical transmission range, and possibly very low loss in the mid-infrared region of the spectrum.[1] In addition, these glasses can be pulled into fibers of extended lengths.[2] We have measured the optical properties of samples of both bulk and fiber zirconium fluoride glass. These properties include the refractive index, absorption and scattering in bulk samples, fiber total loss spectra, fiber scattering loss, and radiation effects. Fibers were pulled from the bulk glass using both the single crucible technique (which produced uncladded fibers), and from preform rods (which produced glass cladded fibers).

The basic glass composition was:
53.0 ZrF_4 19.0 BaF_2 - 5.0 LaF_3 - 3.5 AlF_3 - 19.4 LiF (mole %). To this was added various amounts of PbF_2. The glass was synthesized using all reagent grade component fluorides with some ammonium bifluoride. Melting was carried out in platinum crucibles loosely covered with platinum foil, under a dry argon atmosphere. The glass was melted at 800°C for 1 hour and subsequently was annealed at 250°C inside the melting crucible. The glass has a high activation energy for viscous flow, indicating a high degree of polymerization.[3] Glass containing about 5% PbF_2 was used for the core glass of the fibers, and glass without PbF_2 was used for the cladding glass. These two glasses show similar thermal expansion coefficients.

For the glass containing 5% PbF_2 the expansion coefficient is 1.34 x 10^{-5}/°C and the glass without PbF_2 has an expansion coefficient of 1.41 x 10^{-5}/°C.[4]

The refractive index spectra for the bulk samples were determined by measuring the refraction of a laser beam through prisms of the glasses. These results are shown in Figure 1. The upper curve shows the index of the glass containing about 5% PbF_2. The index in the visible region is about 1.530, dropping to about 1.500 at 3 microns. The lower curve shows the index of the glass without PbF_2. The index is about 1.515 in the visible, dropping to about 1.485 at 3 microns. The middle curve shows the index of a glass containing an intermediate amount, about 3.7%, of PbF_2. The index difference between the core glass (5% PbF_2) and the cladding glass (no PbF_2) is about 1%, corresponding to a fiber N.A. of .20. This is a relatively high value, and should be compared to an N.A. of .123 obtained by varying the BaF_2 content.[5]

Uncladded fibers were pulled from the core glass using the single crucible technique. The fibers had a diameter of about 100 microns and lengths of up to 1000 meters. Glass cladded fibers were pulled from the core and cladding glasses using the preform technique. These fibers also had a diameter of about 100 microns and lengths of up to 30 meters. The total loss of these fibers was measured with the experimental set-up shown in Figure 2. Chopped infrared radiation from a Nernst glower passed through a monochromator and order blocking filters. The radiation was focused onto the fiber using concave mirrors, with a launch N.A. of .03. The radiation from the output end of the fiber was detected with a cooled InSb detector, and the signal passed through a low noise pre-amp and into a lock-in amplifier. The cut-back method was used to determine the fiber loss. The results from these measurements are shown by the upper curves in Figure 3. Both the cladded and uncladded fibers

showed very high losses of about 10 dB/meter. The peak due to water impurity corresponds to about 6 ppm of water, as determined by using the absorption coefficient of OH in silica based glass as a reference. The fibers also showed a large amount of scattering. It should be emphasized that no attempt has been made so far to purify the glass or reduce the scattering.

The scattering loss of the cladded fibers was measured using an integrating sphere detector and an argon-ion laser. The results are shown in Figure 3. The scattering loss is very high, around 100 dB/meter in the visible region, and has an inverse square wavelength dependence. The scattering is probably due to phase separation occuring during the fiber drawing process due to inadequate temperature control. As shown in Reference 6, scattering centers whose size is large compared to the wavelength but having an index similar to that of the surrounding glass (such as microcrystallites) would be expected to result in a scattering loss with the observed wavelength dependence.

In order to better understand the loss mechanisms of the fibers, the absorption and scattering losses of bulk samples were measured. The absorption was determined using laser calorimetry, and these results are shown in Figure 3. In the visible region, the absorption loss is several decibels per meter, due to the strong absorption bands that the transition metal impurities show in this spectral region. The loss drops to about .6 dB/meter at 1.06 microns, and increases again at 3.4 microns due to water impurity. The concentrations of the main transition metal impurities in our glass are also shown in Figure 3. The concentrations of Ni and Cr were estimated using the results of Reference 7 for the absorption coefficients of transition metal impurities in fluoride glass. The concentrations of Cu, Fe, and Ce were determined using d.c. plasma emission spectroscopy. The impurity levels are

all several parts per million; however, no attempt has been made so far to purity our glass, which used reagent grade starting materials.

The scattering loss of bulk samples was measured using an argon-ion laser, a HeNe laser, and a silicon photodiode detector. The laser beam was focused into the sample and positioned so as to avoid passing through the few small inclusions present in the sample. The scattering from a small solid angle was detected at an angle of 90° to the incident laser beam, and the equations given in Reference 8 were used to calculate the total scattering loss. The scattering loss for pure fused silica (Suprasil 1) was also measured for comparison. The results shown in Figure 4 are for a sample containing no PbF_2. The loss at .6328 microns is 4.4 dB/km, and the depolarization ratio is about .20. This loss is more than an order of magnitude lower than previously reported values for zirconium fluoride based glass,[5] and comparable to the loss of fused silica, although slightly greater than the theoretical predictions.[9] The loss follows a λ^{-4} wavelength dependence, typical of Rayleigh scattering. At 4 microns, where the minimum of the total loss is expected to occur, the extrapolated scattering loss is 2.8×10^{-3} dB/km. These results indicate that the high scattering loss seen in the fibers is introduced during the fiber drawing process.

For most applications, it is sufficient that a glass show high transmission only in its natural state. However, for some applications it is also necessary that the glass show high transmission after being exposed to high doses of ionizing radiation. To determine the radiation hardness properties of our glass, bulk samples were irradiated at a dose of 10^7 rads (Si) by a ^{60}Co source. The irradiated samples had a light tan color, although no change in their infrared transmission was seen. The u.v., visible, and infrared transmission spectra of the irradiated samples are shown in Figure 5. In contrast to silica based glasses which show absorption peaks when exposed

to irradiation due to color centers, the zirconium fluoride glass shows a shift of its u.v. edge towards longer wavelengths with increasing dosage. This shift is less pronounced for glass without PbF_2, and is the least for glass containing 5% CeF_3, as can be seen in Figure 6. Laser calorimetry at 3.4 microns indicated no change in the infrared absorption for the irradiated sample, although data from irradiated fibers is needed to determine the true radiation hardness properties of the glass. The Raman spectra of the irradiated glass, which indicates some structural damage, is given in Reference 10.

In conclusion, we have produced substantial lengths of both cladded and uncladded fiber from zirconium fluoride based glass. Although the total loss for the fibers is relatively high at the present time, we believe that better temperature control during fiber drawing and purification of the starting materials will result in low loss fibers. The low scattering loss measured in the bulk samples indicates potentially very low fiber loss in the infrared.

REFERENCES

1. Drexhage, M. G. and Quinlan, K. P. In "Advances in Ceramics," Vol. 2 (1981) p. 57 (B. Bendow and S. Mitra, eds). The American Ceramic Society, Inc., Columbus, OH.
2. Ginther, R. J. and Tran, D. C., Technical Digest, IOOC Meeting, April 1981, San Francisco, CA.
3. Tran, D. C., Ginther, R. J., and Shiraishi, Y. to be published in Materials Research Bulletin.
4. Tran, D. C., Ginther, R. J., Sigel, G. H., and Levin, K. H., OFC Meeting, April 1982, Phoenix, AZ.
5. Mitachi, S. and Miyashita, T., Electron. Lett., 18, 170 (1982).
6. Harrington, J. A. and Sparks, M., unpublished.
7. Ohishi, Y., Mitachi, S., and Kanamori, T., Jap. J. of App. Phys., 20, L787 (1981).
8. Laybourn, P. J. R., Dakin, J. P., and Gambling, W. A., Opto-Electr. 2, 36 (1970).
9. Poignant, H., Electronics Lett., 17, 973 (1981).
10. Fiedler, K. H., Levin, K. H., and Tran, D. C., Phys. and Chem. of Glasses, to be published, Dec. 1982.

FIGURE CAPTIONS

Figure 1 Refractive index spectra of zirconium fluoride based glasses.

Figure 2 IR fiber spectral loss measurement system.

Figure 3 Loss spectra for zirconium fluoride glass fibers.

Figure 4 Scattering loss spectrum for bulk zirconium fluoride glass.

Figure 5 Absorption spectra of irradiated zirconium fluoride glass.

Figure 6 UV edge of irradiated zirconium fluoride glasses.

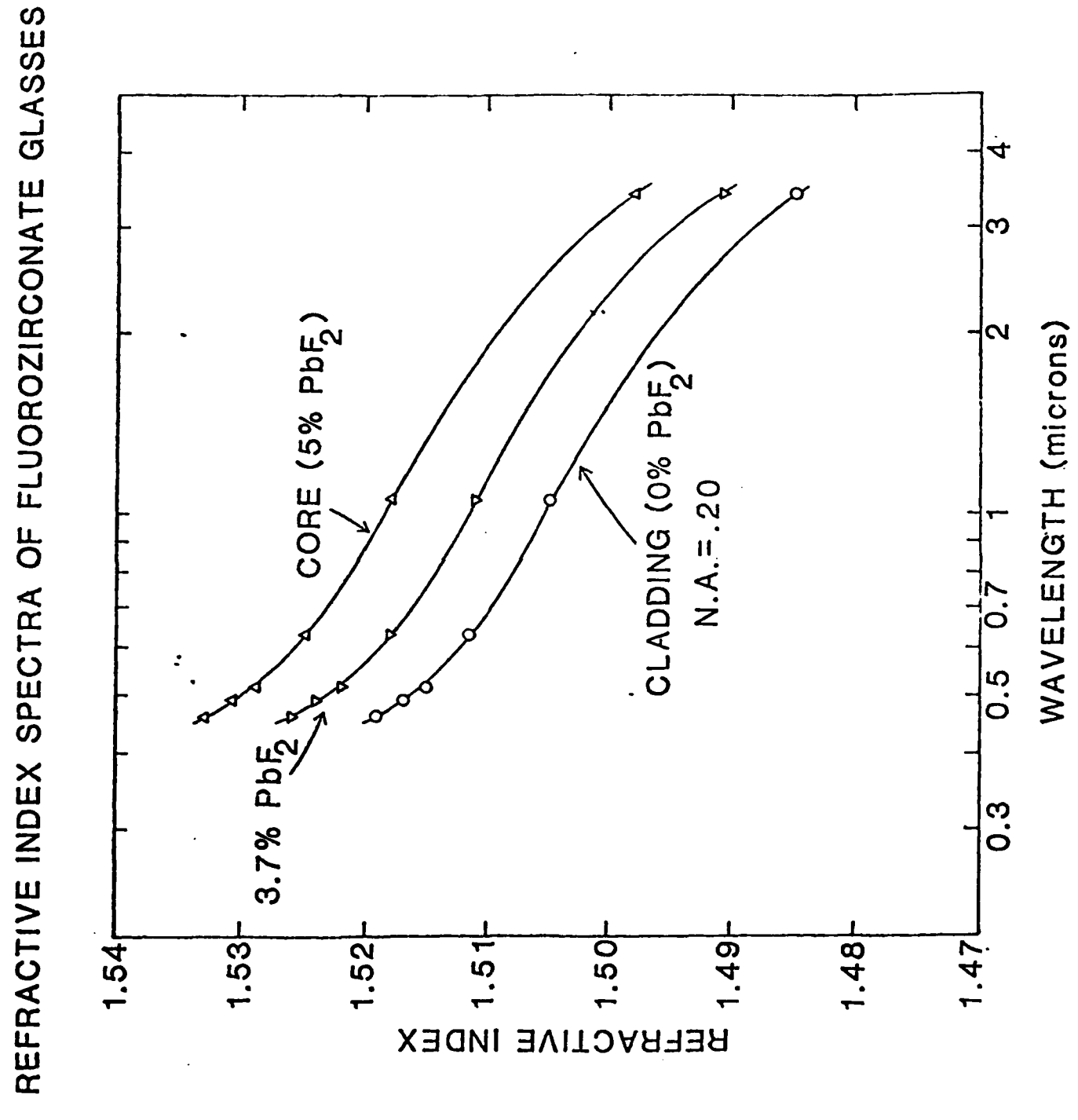
REFRACTIVE INDEX SPECTRA OF FLUOROZIRCONATE GLASSES
REFRACTIVE INDEX
1.54
1.53
1.52
1.51
1.50
1.49
1.48
1.47
WAVELENGTH (microns)
0.3
0.5
0.7
1
2
3
4
CORE (5% PbF2)
3.7% PbF2
CLADDING (0% PbF2)
N.A. = .20

Figure 1

IR FIBER SPECTRAL LOSS MEASUREMENT SYSTEM

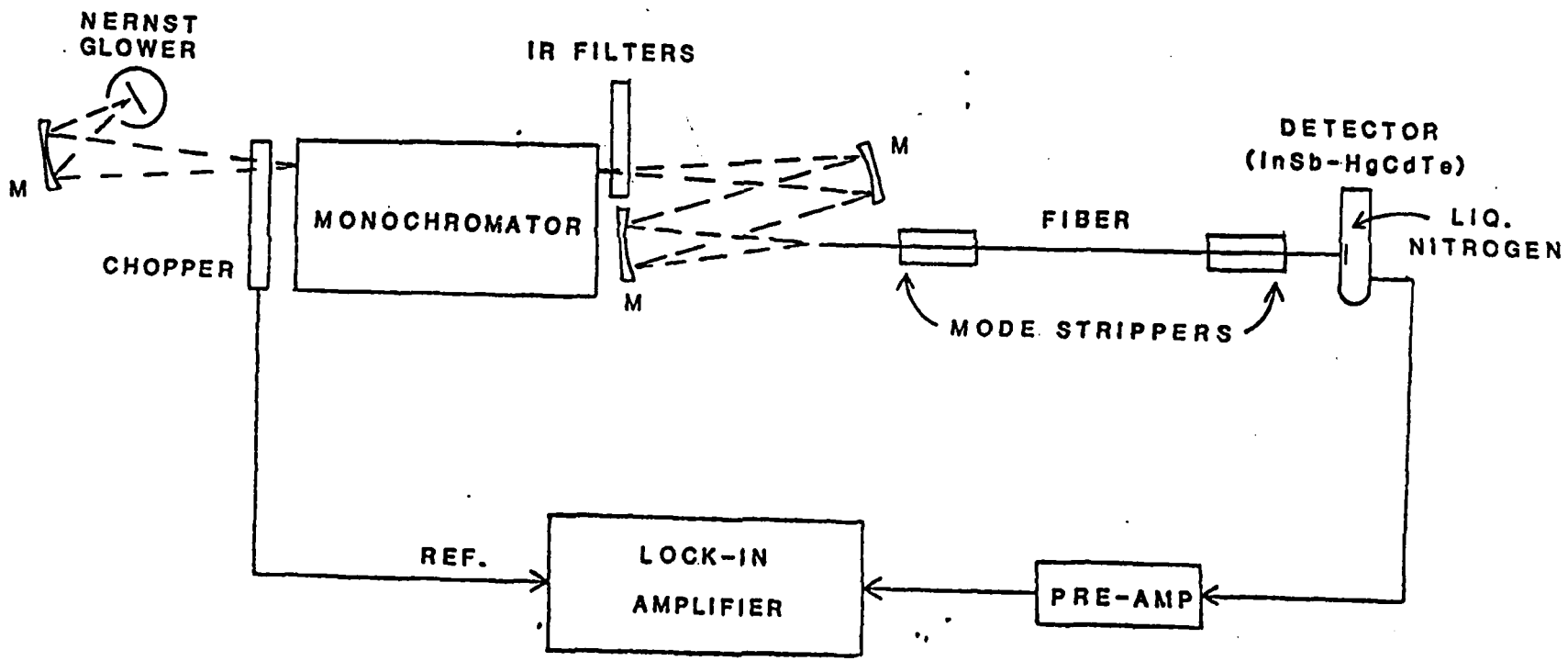

Figure 2.5

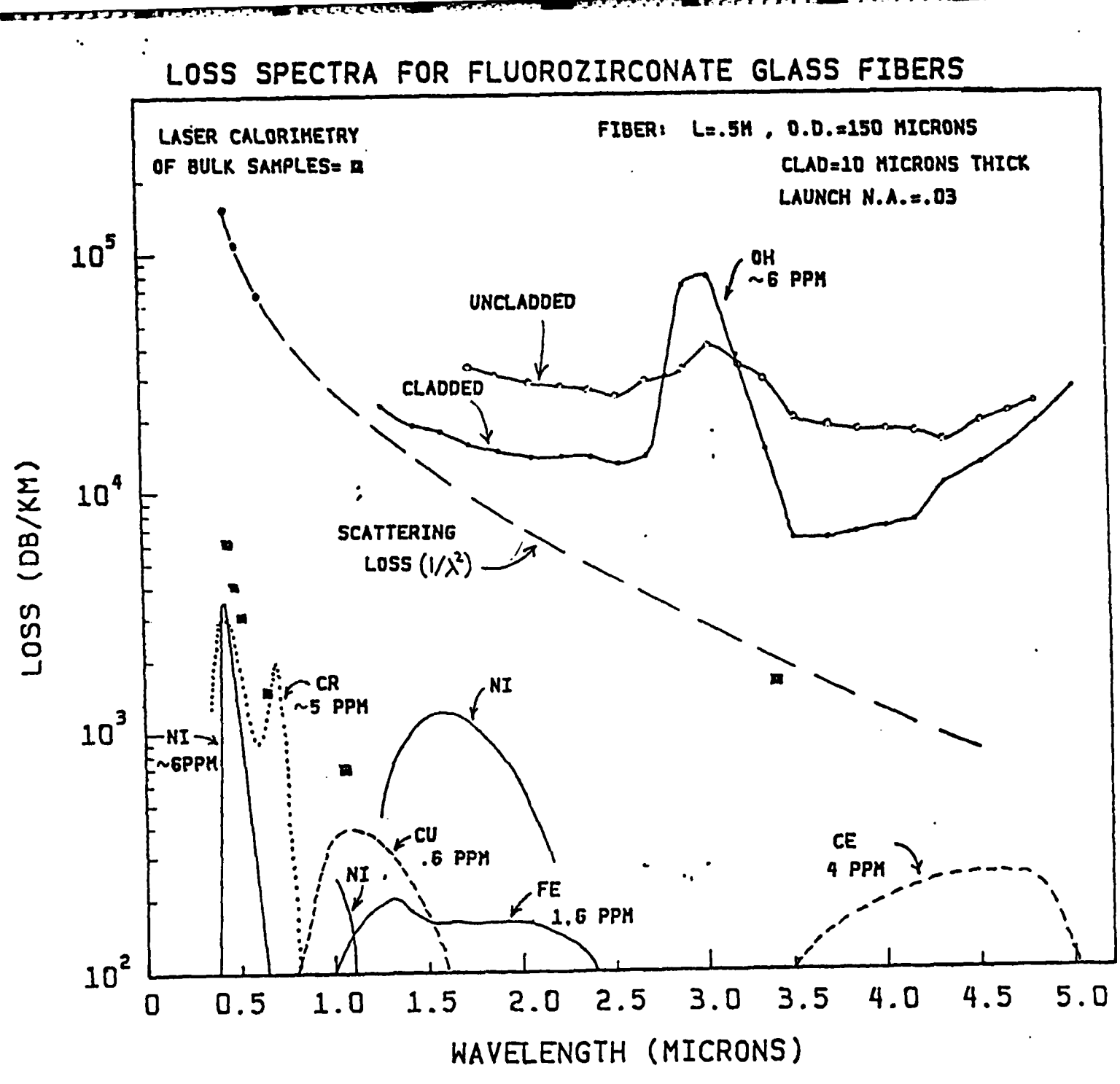
LOSS SPECTRA FOR FLUOROZIRCONATE GLASS FIBERS
LASER CALORIMETRY
OF BULK SAMPLES= ■
FIBER: L=.5M , O.D.=150 MICRONS
CLAD=10 MICRONS THICK
LAUNCH N.A.=.03
UNCLADDED
CLADDED
OH
~6 PPM
SCATTERING
LOSS (1/λ²)
CR
~5 PPM
NI
~6PPM
NI
CU
.6 PPM
NI
FE
1.6 PPM
CE
4 PPM
LOSS (DB/KM)
WAVELENGTH (MICRONS)

Figure 3

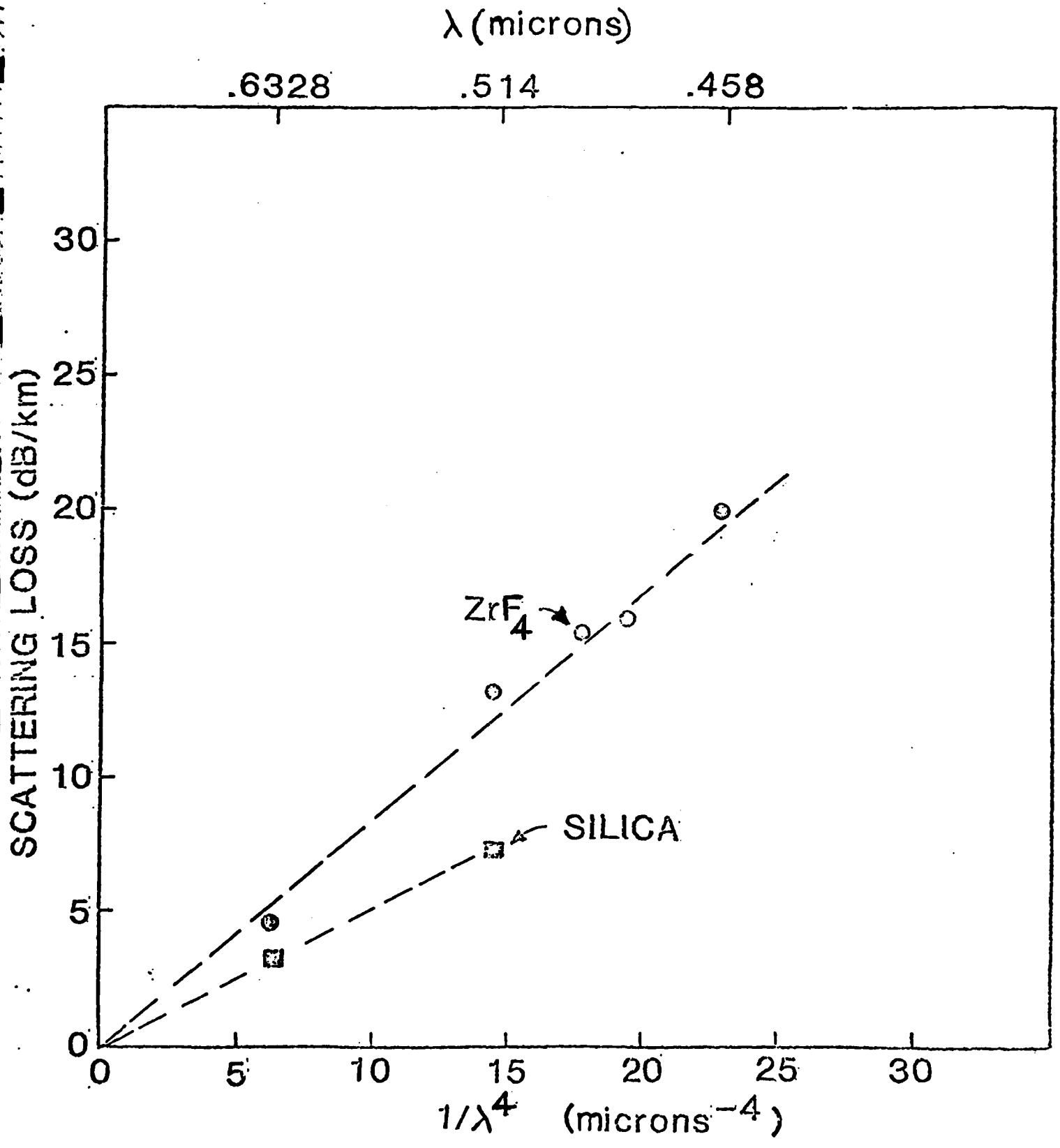
λ (microns)
.6328
.514
.458
SCATTERING LOSS (dB/km)
30
25
20
15
10
5
0
ZrF4
SILICA
0
5
10
15
20
25
30
1/λ4 (microns−4)

Figure 4

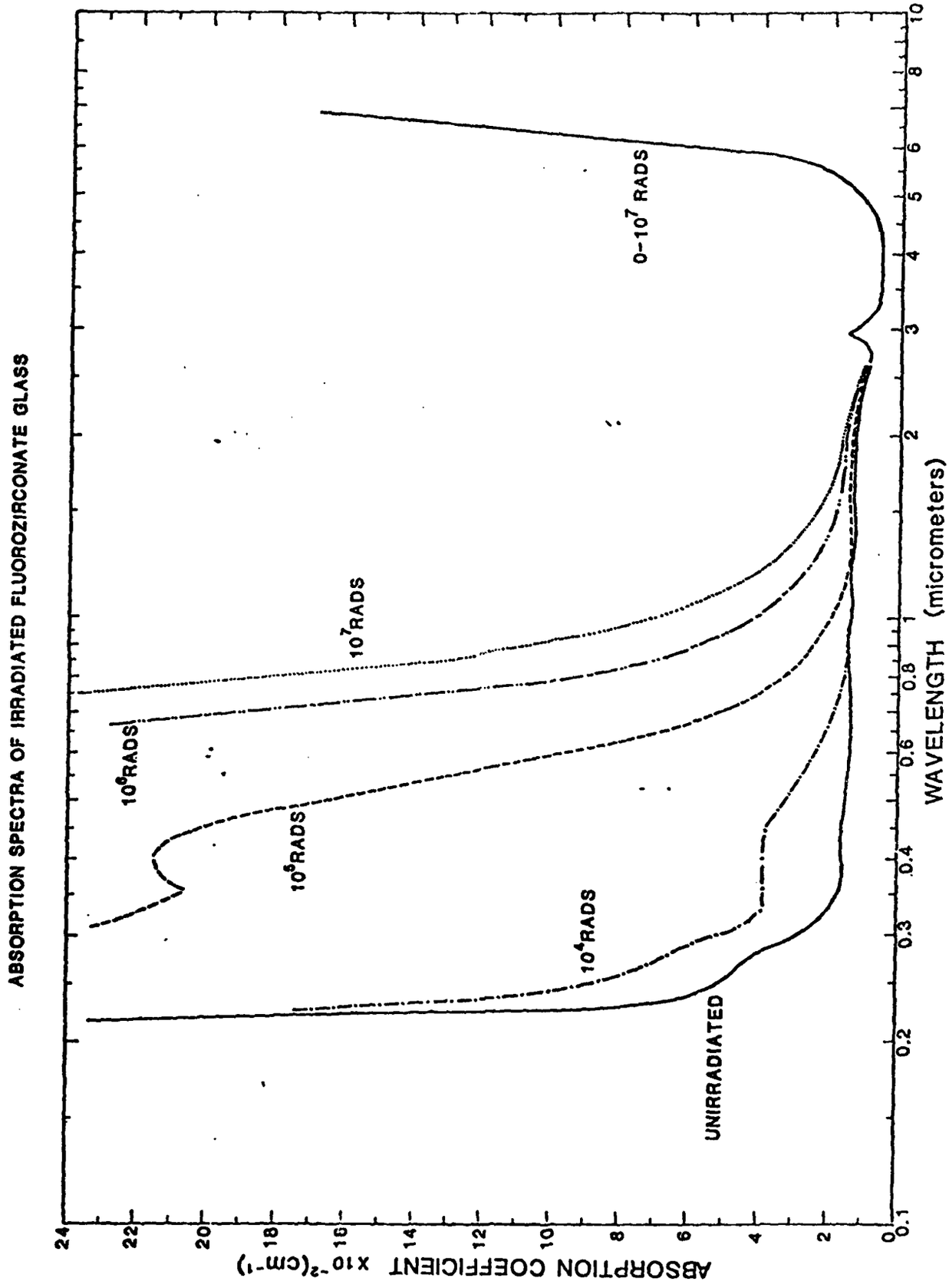
ABSORPTION SPECTRA OF IRRADIATED FLUOROZIRCONATE GLASS
ABSORPTION COEFFICIENT x10⁻²(cm⁻¹)
WAVELENGTH (micrometers)
0-10⁷ RADS
10⁷RADS
10⁶RADS
10⁵RADS
10⁴RADS
UNIRRADIATED

Figure 5

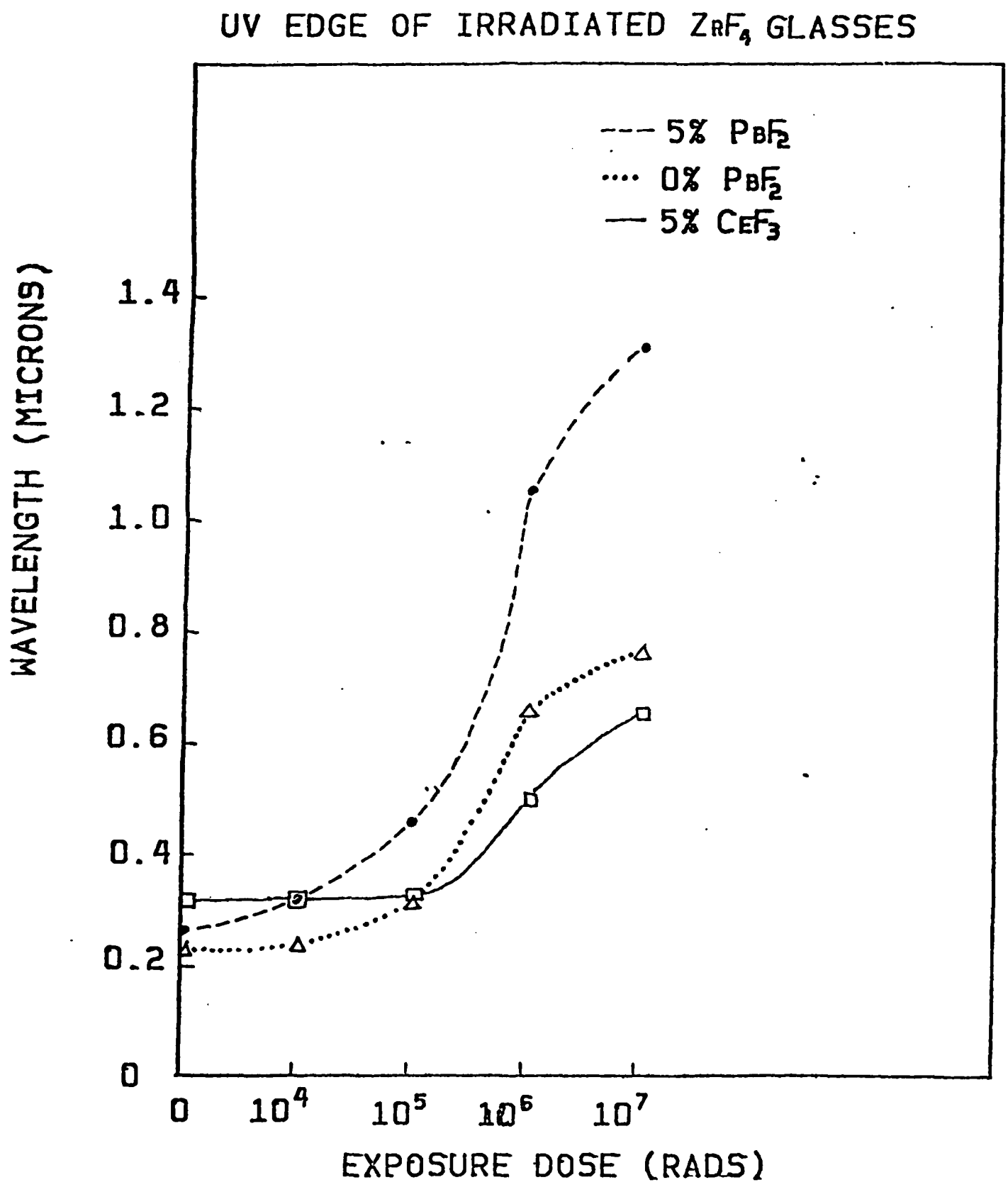
UV EDGE OF IRRADIATED ZrF_4 GLASSES
--- 5% PbF_2
···· 0% PbF_2
— 5% CeF_3
WAVELENGTH (MICRONS)
1.4
1.2
1.0
0.8
0.6
0.4
0.2
0
0
10^4
10^5
10^6
10^7
EXPOSURE DOSE (RADS)

Figure 6

To be published in "Physics and Chemistry of Glasses" Dec, 1982

RAMAN SPECTRUM OF IRRADIATED FLUORIDE GLASS

K. H. Fiedler,* K. H. Levin,** and D. C. Tran
Naval Research Laboratory
Washington, D. C. 20375

Abstract

The Raman spectra have been measured for both irradiated and unirradiated samples of zirconium fluoride-based glass. The spectrum of the irradiated sample showed several new bands and an intensification of weak bands in the low frequency region suggesting that some structural damage of the glass network due to the irradiation had occurred.

* Georgetown University
Washington, D. C. 20057

** Sachs/Freeman Associates, Inc.
Bowie, MD 20715

I. INTRODUCTION

There has recently been much interest shown in the fluoride glasses due to their wide optical transmission range, and possibly very low loss in the mid-infrared region of the spectrum.[1] Of particular interest are the zirconium fluoride-based glasses, which recently have been shown capable of being pulled into fibers of extended lengths.[2] The structure of these glasses, as determined by infrared and Raman spectra, is believed to consist of crosslinked polymer-like chains, with most of the fluorine atoms occupying non-bridging positions in the chains.[3] As is known from studies on silica-based glasses,[4] irradiation can cause changes in the optical absorption and structure of the glass. In this paper, we have used Raman scattering to determine the effect of irradiation on the structure of zirconium fluoride-based glass. The results of infrared transmission measurements on irradiated samples will be reported elsewhere.[5]

II. EXPERIMENTAL

Raman scattering spectra were taken of irradiated and unirradiated samples of fluoride glass having the following composition:
53.0 ZrF_4 - 19.0 BaF_2 - 5.0 LaF_3 - 3.5 AlF_3 - 19.5 LiF (mole %). The glass was synthesized using all reagent grade component fluorides with some ammonium bifluoride. Melting was carried out in platinum crucibles loosely covered with platinum foil, under a dry argon atmosphere. The glass was melted at 600°C for 1 hour and subsequently annealed at 250°C inside the melting crucible. The glass showed a high activation energy for viscous flow, indicating a high degree of polymerization.[6] The irradiation, at a 1 MeV gamma-ray dose of 10^7 rads (Si), was carried out using a ^{60}Co source, at a dose rate of 1.2×10^4 rad/min. After irradiation, the sample had a light tan color, probably due to the formation of color centers.[4]

The Raman spectra were obtained using a Spex 1401 double monochromator with holographic gratings peaked for performance between 600 and 800 nm. The detector was a cooled photomultiplier tube used together with a Spex DPC 2 photon counting equipment. The Spex double monochromator was automated with an Intel digital microprocessor interfaced to a Digital VT/78 video data minicomputer. The light from an Argon ion laser (Coherent Radiation CR-2: Wavelength 514.5 nm, power 800 mW) was focused on the samples and the 180° backscattered light was collected. This technique had to be used because the samples showed quite different features with respect to shape, surface condition and light absorption. All experiments were performed using a scrambler in front of the entrance slit of the monochrometer to eliminate the polarization dependence of the gratings. Because of the weak signals received the spectra were recorded with fairly wide slit settings. The resulting resolutions were 3 cm^{-1} in the low frequency region (25-185 cm^{-1}) and 5 cm^{-1} in the frequency range 150-870 cm^{-1}. The Raman spectra were obtained by co-adding several runs.

III. RESULTS

Considering the chemical composition of the examined samples our Raman scattering results agree very well with those of Almeida and Mackenzie[3], see Table 1 and Figures 1 and 2. The spectrum of the unirradiated material (Figure 2) shows the composition related very intense band in the expected frequency range at 579 cm^{-1} with a half width of 56 cm^{-1}. This dominant band was assigned[3] to the totally symmetric stretching vibration ν_s (Zr - F_{nb}) involving only nonbridging fluorine atoms F_{nb}. As known from hydrogen bonding in organic polymers[7] the stretching vibration frequencies of bonds affected by bridging effects will appear at lower wave numbers. Almeida et al.[3] assigned the band at 479 cm^{-1} to the symmetric stretching vibration SS (Zr - F_b) of Zr - F - Zr bonded fluorine atoms F_b. Our low frequency spectrum of the unirradiated material (Figure 1) shows that the

unassigned band near 50 cm^{-1} [3] consists of two sharp but weak bands at 46 and 49 cm^{-1} as well as three very weak bands at about 40, 60, and 75 cm^{-1}.

The effects of the gamma irradiation were mainly expressed by the appearance of strong bands in the low frequency region below 100 cm^{-1}. All five bands seen in the unirradiated glass are still present in the spectrum of the irradiated sample (Figure 1), although their intensities have increased substantially.

At higher frequencies above 150 cm^{-1} (Figure 2) a band at 273 cm^{-1} -- not observed by Almeida et al.[3] -- is no longer present in the spectrum of the irradiated glass, which shows new bands centered at 192 and 260 cm^{-1}. The dominant bands at 479 and 581 cm^{-1} show the same relative intensities as for the unirradiated sample.

IV. CONCLUSION

The intensification of weak bands and the appearance of new bands for the irradiated sample suggest that some structural damage of the glass network has occurred. The dramatic difference between the spectra below 100 cm^{-1} of the unirradiated and irradiated materials can be interpreted as an activation process of localized modes which possibly are skeletal and librational vibrations of the polymer-like chains broken by the irradiation. Localization of low frequency modes is also seen in neutron irradiated silica glass.[8] Additional research on materials with systematically varied compositions as well as different degrees of irradiation will give important information about the nature of the irradiated network.

Acknowledgments

The authors are grateful to George H. Sigel, Jr. for his support of this work.

References

1. Drexhage, M. G. and Quinlan, K. P. In "Advances in Ceramics," Vol. 2 (1981) p. 57 (B. Bendow and S. Mitra, eds.). The American Ceramic Society, Inc., Columbus, Ohio.
2. Ginther, R. J. and Tran, D. C. Technical Digest, IOOC Meeting, April 1981, San Francisco, CA.
3. Almeida, R. M. and Mackenzie, J. D. J. Chem. Phys., 74 (1981) 5954.
4. Friebele, E. J. and Griscom, D. L. In "Treatise on Materials Science and Technology," Vol. 17 (1979), p. 257 (M. Tomozawa and R. Doremus, eds.). Academic Press, N. Y.
5. Levin, K. H., Tran, D. C., Ginther, R. J., Sigel, G. H., and Fiedler, K. H. Proceedings of the Symposium on Halide and Other Non-Oxide Glasses. Cambridge, England March 1982.
6. Tran, D. C., Ginther, R. J., and Shiraishi, Y., to be published in Materials Research Bulletin.
7. Bessler, E. and Bier, G. Makromol. Chem. 122 (1969) 30.
8. Bates, J. B., Hendricks, R. W. and Shaffer, L. B. J., Chem. Phys. 61 (1974) 4163.

Table 1. Band frequencies and intensities of the unirradiated and irradiated fluoride glass.

Unirradiated Sample $\nu(cm^{-1})$	Irradiated Sample $\nu(cm^{-1})$
38 sh	39 w
46 w	46 s
49 w	49 w
60 vw	61 w
75 vw	75 s
	192 m
273 w	260 w
392 w	393 w
479 m	479 m
579 s	581 s

Nomenclature: ν-frequency in cm^{-1}; s-strong; m-medium; w-weak; v-very; sh-shoulder; b-broad.

Figure Captions

Figure 1: Low frequency Raman spectra of irradiated and unirradiated fluoride glass.

Figure 2: High frequency Raman spectra of irradiated and unirradiated fluoride glass.

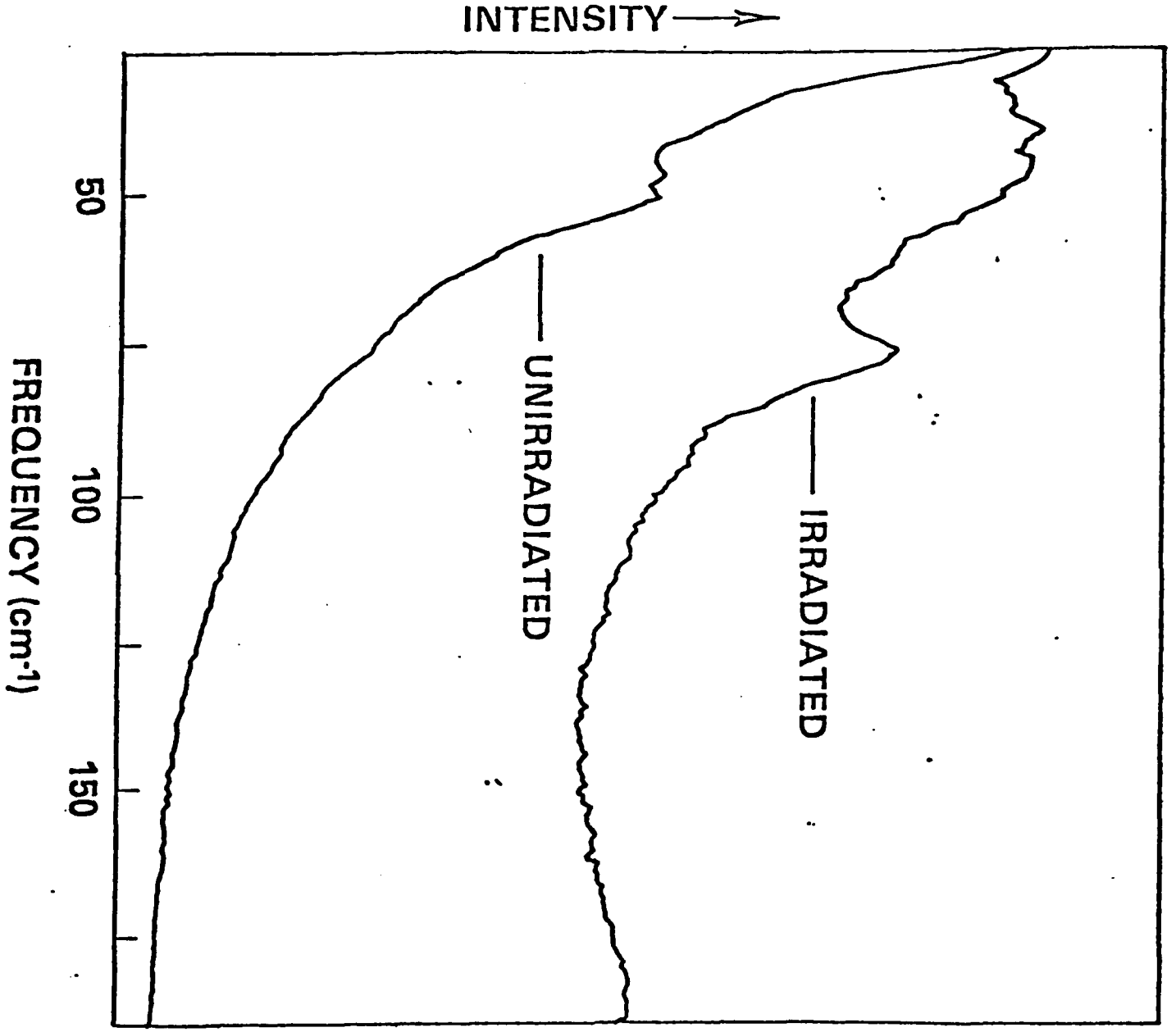
INTENSITY
50
100
150
FREQUENCY (cm-1)
UNIRRADIATED
IRRADIATED

Figure 1

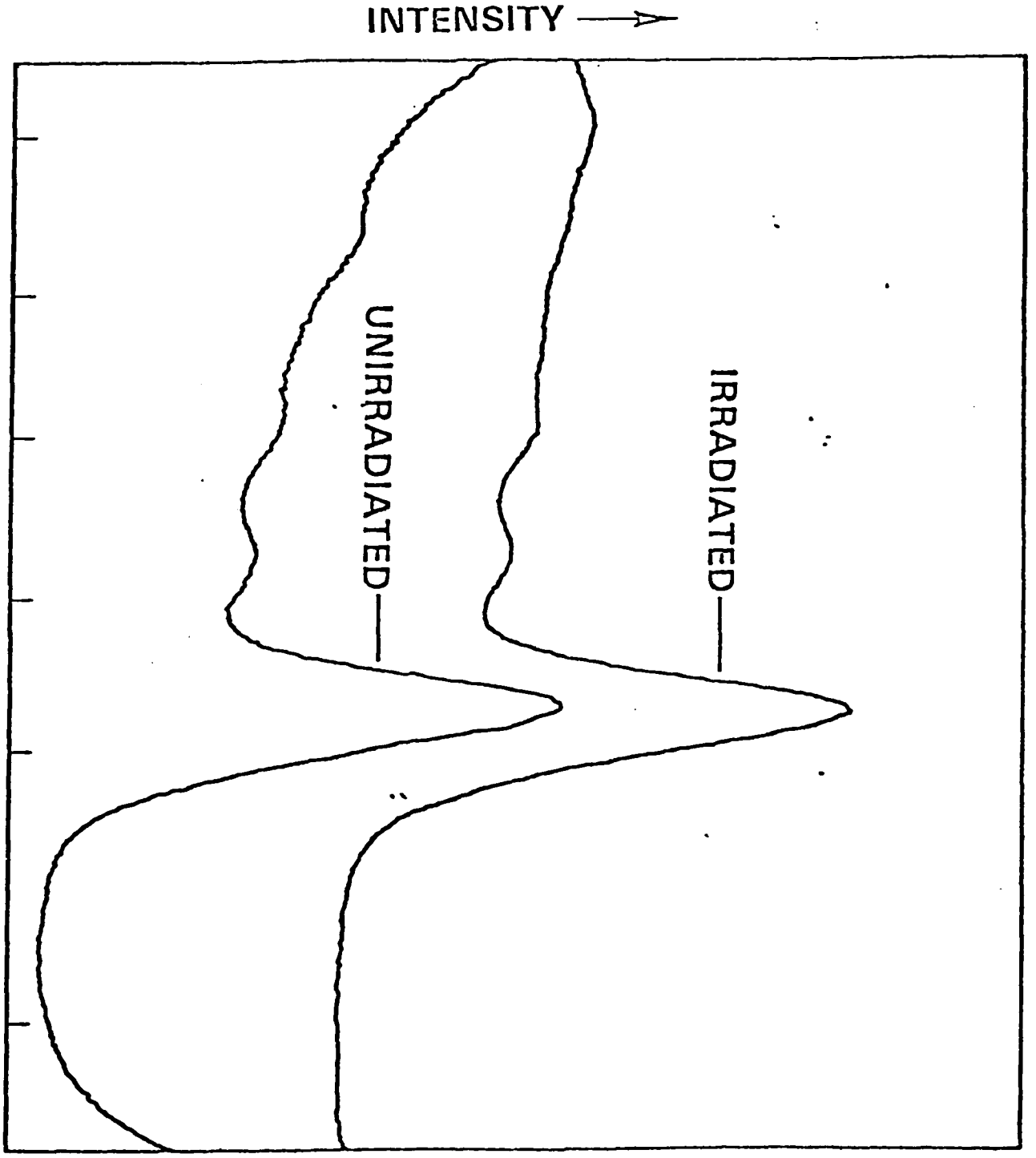
INTENSITY
UNIRRADIATED
IRRADIATED
200
400
600
800
FREQUENCY (cm-1)

PULSE BROADENING IN OPTICAL FIBERS

Herbert B. Rosenstock*
Naval Research Laboratory
Washington, DC 20375

ABSTRACT

A light pulse transmitted through a fiber will spread even if the source is perfectly monochromatic and even if the fiber is thin enough to transmit one mode only. The effect can be attributed to the extended frequency spectrum that is associated with a finite pulse.

Here, this effect is analyzed mathematically. We wind up with a relation between the initial pulse width τ and the maximum range of transmission L^* in the form

$$L^* = a\ \tau^2$$

where a depends on the physical parameters of the problem. This implies that maximizing the amount of information transmitted, which demands keeping τ small, precludes maximizing the transmission distance. One numerical example suggests that with a bit-rate of 10 gigahertz, the transmission range is limited to 100 kilometers.

*Sachs/Freeman Associates, Bowie, MD 20715

I. Introduction

Light pulses transmitted through an optical fiber, like all signals used for communication, deteriorate with distance. There are at least three reasons for this:

1. Multiple modes. Different waveguide modes travel at different speeds, and the total pulse is therefore distorted (spread out) as it moves down the fiber.[1]
2. Finite linewidth. Different frequencies contained in the light source travel at different speeds, details depending a) on the optical properties of the fiber material, and, b) on the radius of the fiber. This again results in distortion of the total pulse.[2]
3. Finite pulsewidth. A pulse of light -- as contrasted to a wave train extending in time from $-\infty$ to ∞ -- is equivalent to many frequencies. This is the true even if the original source is is monochromatic. As in mechanism 2 above, these frequencies travel at different speeds, causing distortion.

Mechanisms 1 and 2 have been amply studied,[3,4] but mechanism 3, though well known from other physical applications of wave propagation,[5] has apparently not been discussed in detail[6] in relation to fiber optics. It is the subject of this paper.

In Section II, the simple theory is presented, resulting in a formal expression for the pulse shape at any point in terms of the pulse shape at the origin. In Section III, this is evaluated for a Gaussian pulse, the only shape for which we were able to obtain an analytical solution. The practical implications of this solution are discussed in

Section IV. Section V discusses other pulse shapes and relates their properties to those of the Gaussian previously solved. Results are summarized in Section VI.

II. Theory

We consider a signal of the form

$$f(t) = e^{2\pi i \nu_0 t} P(t) \tag{1}$$

where ν_0 is the frequency produced by our light source (laser) and P(t) is a pulse, centered about t=0 and small for $|t|<\tau$. τ may be called the pulse width. The reader may want to glance at Figure 1 for examples of P(t) we will consider later in detail. Since f(t) does not extend uniformly from $t=-\infty$ to ∞, it is not a plane wave; but according to Fourier's theorem it can be expanded in plane waves,

$$f(t) = \int_{-\infty}^{\infty} d\nu\, e^{2\pi i \nu t} g(\nu) \tag{2}$$

where $g(\nu)$ can be considered a known function; it is in fact given by

$$g(\nu) = \int_{-\infty}^{\infty} dt\, e^{-2\pi i \nu t} f(t). \tag{3}$$

With the use of (1) and the restriction that P(t) is even about the origin this can be written

$$g(\nu) = 2\int_{0}^{\infty} dt \cos 2\pi s t\; P(t) \tag{4}$$

where

$$s = \nu - \nu_0 . \tag{5}$$

We insert the signal f(t) into a fiber and ask what the signal will look like a distance L away. The answer is obtained by replacing t in (2) by t-(L/v),

where the velocity of propagation v is given by

$$V = C/n(\nu), \tag{6}$$

c is the speed of light in vacuuo, and the index of refraction n(ν) of the material that the fiber is made of is a function of the frequency ν. We thus obtain

$$\bar{f}(t,L) = \int_{-\infty}^{\infty} d\nu\, e^{2\pi i \nu [t - \frac{L n(\nu)}{c}]} g(\nu) \tag{7}$$

for the signal $\bar{f}(t,L)$ that will appear at point L along the fiber. n(ν) can presumably be measured and should be considered known; it can often be adequately approximated by the linear expression

$$n(\nu) = n_o\,(1+\gamma s) \tag{8}$$

where n_o means $n(\nu_o)$, and γ is is a constant; under these circumstances (7) becomes

$$\bar{f}(f,L) = e^{2\pi i \nu_o t'} \int_{-\infty}^{\infty} ds\, e^{2\pi i [t'' s - \beta s^2]} g(\nu) \tag{9}$$

where

$$\left.\begin{aligned} t' &= t - \frac{L n_o}{c} \\ t'' &= t - \frac{L n_o}{c}(1+\beta) \end{aligned}\right\} \tag{10}$$

and

$$\beta = n_o \gamma L/c \tag{11}$$

is another constant. The case where s in (8) is replaced by s^2 would also be of interest, but is not considered here.

III. Gaussian Pulse

The only pulse shape for which we have been able to evaluate (9) in closed form is the Gaussian,

$$P(t) = e^{-(t/\tau)^2}/\tau\sqrt{\pi} \tag{12}$$

In that case (4) is

$$g(\nu) = e^{-(\pi\tau\delta)^2} \tag{13}$$

and (9) becomes

$$\bar{f}(t,L) = e^{2\pi i\nu_0 t'}\sqrt{\pi}\, e^{-(t''\pi)^2}/\rho \tag{14}$$

with

$$p^2 = (\pi\tau)^2 + 2\gamma\beta i \tag{15}$$

The imaginary part of p can be ignored in the denominator of (14), where it cannot affect the pulse shape but can produce at most a constant multiplicative factor; but it must be treated exactly in the exponent. We find

$$e^{-(t''\pi/\rho)^2} = e^{-(t''/\bar{\tau})^2} e^{i\sigma(t'/\tau)^2} \tag{16}$$

where

$$\bar{\tau}(L) = \tau\sqrt{1+\sigma^2} \tag{17}$$

and

$$\sigma = 2L n_0\gamma/\pi c\tau^2. \tag{18}$$

In (16), we can again ignore the second term, a complex modulating factor of modulus unity. With these simplifications, (14) becomes

$$\bar{f}(t,L) = e^{2\pi i \nu_0 t'} e^{-(t''/\bar{\tau})^2} / \bar{\tau}\sqrt{\pi}. \qquad (19)$$

We can ignore the difference between t", t', and t -- they all represent time, and differ only in the choice of origin. Thus (19) looks very much like the incoming signal (1), (12): a Gaussian modulated by a plane wave of frequency ν_0. The major difference is that the width of the Gaussian has increased from τ to $\bar{\tau}$ given by (17).

IV. Broadening with Distance: Discussion

We have shown that a Gaussian pulse of initial width τ will remain Gaussian but attain a width $\bar{\tau}$ given by (17) and (18) after traveling a distance L through a fiber; γ is related to the optical dispersion,

$$\gamma = dn/d\nu \qquad (20)$$

We see that for small L, the spread is slow, but for large enough L the width becomes proportional to L itself. Furthermore, for large L the final width $\bar{\tau}(L)$ becomes inversely proportional to the initial width τ: The final pulse width is larger for pulses that start out narrower, a result that may seem surprising. The crossover point at which two pulses initially of width τ_1 and τ_2 are equal in width is seen to occur at distance $L = \pi c \tau_1 \tau_2 / 2 n_0 \gamma$

There are several ways of extracting information from (17), (18). The easiest way is to ask for the distance L^* in which the width will increase by a factor of $\sqrt{2} = 1.41$. This is seen from (17) to be given by $\sigma = 1$, or according to (18),

$$L^* = \pi c \tau^2 / 2 n_0 \gamma . \qquad (21)$$

Roughly speaking, L^* is the distance at which the spread becomes rapid, soon to be intolerable. Again, the appearance of τ^2 on the righthand side suggests that one doesn't accomplish much by making the initial pulse very narrow -- catastrophic spreading will start sooner.

Let us work out one numerical example. The following numbers have been reported[7] for SiO_2 doped with 4.1 mol % GeO_2 at a wavelength of $\lambda = 1$ micrometer:

$$n_0 = 1.457, \quad \lambda (dn/d\lambda) = -.0123 \qquad (22)$$

From the last figure and our (20) it follows that $\gamma = .0123\ \lambda/c$. (21) then gives

$$L^* = 8 \times 10^{24}\ \tau^2 \text{ meters}$$

where the pulsewidth τ is in seconds. So if we take

$$\tau = 10^{-9} \text{ sec}$$

(bitrate of 1 gigahertz), we obtain

$$L^* = 8000 \text{ km}$$

for the distance beyond which pulse spread is unacceptable. For a pulsewidth

$$\gamma = 10^{-10}\ \text{sec}$$

that distance would be only

$$L^* = 80\ \text{km}.$$

For halide glasses such as LiF or CsF[8] or KRS-5[9], and at longer wavelengths, γ and also n_0 are often larger and L^* therefore turns out to be smaller, by factors ranging from 2 to 20.

Another method of analyzing our results (17), (18) is to ask for the initial width τ that is required so that the final width at distance L should not exceed a specified $\bar{\tau}$. (It is, after all, $\bar{\tau}$ at the far end of the fiber that limits the amount of information that can be transmitted, but the initial τ that can be controlled.) To answer this, we square (17), multiply by τ^2, and solve the resulting quadratic equation in the variable τ^2, obtaining

$$2\gamma^2 = \bar{\tau}^2 \pm \sqrt{\bar{\tau}^4 - 4a^2L^2} \tag{23}$$

where

$$a = 2n_0\gamma/\pi c \tag{24}$$

For the desired $\bar{\tau}$ to be attainable, the solution must be real; that is, we must have

$$\bar{\tau} \geq \sqrt{2aL} \quad . \tag{25}$$

Narrower $\bar{\tau}$ cannot be attained at L by any initial width τ, however small; for wider ones, a range of initial widths, bounded by the two solutions of (23), is allowed. Furthermore, equ. (23) tells us the initial width needed to attain this minimum possible width $\sqrt{2aL}$ at L: it is $\tau = \bar{\tau}/\sqrt{2} = \sqrt{aL}$. This is a design criterion that is worth restating in words: If you want to transmit for a distance L, do not decrease the initial pulsewidth below $\sqrt{aL}$.

As an example, consider again the material defined by the properties (22); (25) then states that at a distance L = 100 km, pulsewidths smaller than 0.16×10^{-9} sec will be unattainable regardless of how small the initial pulse may be.

V. Other Pulse Shapes

What we should like to do is to repeat the work of Sections III and IV for reasonable pulse shapes P(t) other than Gaussian. To find g(ν) by evaluating (4) is usually easy enough; to carry out (9) and find $\bar{f}(t,L)$ is more difficult. In no other case have we succeeded in doing it analytically. However, (9) does allow us to draw some qualitative conclusions about $\bar{f}$ even when we cannot compute it explicitly.

Accordingly, we present in Figure 1 four different pulse shapes P(t) and the corresponding transforms g(ν). All the P(t) are even about the origin, all share the same (approximate) halfwidth τ, and the last of the four

is the well-discussed Gaussian. They are arranged in increasing order of "smoothness": the first has discontinuities in P(t) itself, the second in the first derivative, the third only in the second derivative, and the fourth has no discontinuities at all. All four of the transform functions $g(\nu)$ are also seen to be symmetric about the shifted origin $s = \nu - \nu_o = 0$ and to take on the value 1 there; but they are seen to be sharper, and to fall off more rapidly, with increasing s, as the smoothness of P(t) increases.

This last conclusion, though here based on only the four examples of Table 1, can be accepted as a general one: it is generally understood that "smooth" functions are "easily" represented by a Fourier expansion, or, conversely, that functions with sharp discontinuities require many frequencies in their Fourier representation. If this is true, then it follows from (9) that smooth functions P(t) will keep their shape longest, whereas the initially non-smooth or discontinuous ones -- the ones near the top of figure 1 -- will spread more rapidly. (In detail, this argument is based on the observation that the spreading of the pulse is based on the βs^2 term in (9); if $g(\nu)$ is sharply centered about $s = 0$ and falls off rapidly from there, the contribution of the s^2 term will be negligible and (9) will, except for the trivial difference between t, t', and t", be identical with the initial pulse shape (2)).

Two conclusions can be drawn from this. First, the results of Sections III and IV, which apply exactly to initially Gaussian pulses, can serve as limits for other pulse shapes: for a non-Gaussian pulse, ratio $\overline{\tau}(L)/\tau$ of

width at point L to initial width will be somewhat larger than (17); similarly the "critical distance" L^* by which the pulsewidth increases by a factor of 1.41 will be somewhat smaller than in (21) or the subsequent example. Second, to the extent that pulse shapes can be controlled in a practical fiber-optic system, they should be designed to be as nearly Gaussian as possible, or, if it is not possible, should be smooth rather than have sharp edges or corners.

VI. Summary

We have considered one of the several possible mechanisms that contribute to the broadening of a light pulse being transmitted along an optical fiber. The mechanism is related to the finite width of the pulse, which implies a spectrum of frequency components (even though the original light source may be monochromatic). We were able to obtain a general expression (9) for the pulse shape at any point L, evaluate it in closed form for Gaussian pulses (Eqs. (17) and (19)) and establish a quantitative relations (21) or (25) between initial pulse width, physical parameters describing the fiber material, and transmission distance beyond which broadening is unacceptable. For non-Gaussian initial shapes, we showed that this last relationship somewhat overestimates that maximum distance.

Two of our analytical results may seem surprising when verbalized. First, it is not true that narrow pulses remain comparatively narrow, and wide ones comparatively wide. Rather, initially narrow ones eventually become wider than initially wide ones. Second, it is impossible to simultaneously maximize both the amount of information transmitted per unit time

and the distance of transmission: naively, one might expect to accomplish both by making the initial pulse as narrow as possible, but this, as we have seen, in fact reduces the distance in which unacceptable broadening is produced.

The effect is well known in other fields of physics and engineering, and not hard to treat mathematically. It therefore seems puzzling that it has, apparently, not been considered in connection with fiber optics. One reason may be the comparative smallness of the effect: One (non-conclusive) example suggests that the effect becomes catastrophic only after more than 1000 km of transmission in SiO_2 glass, although the distances may be smaller for halide glasses. Today, other difficulties preclude transmission over distances that large. Nonetheless, the effect may become important in the future, as transmission over very long distances is seriously contemplated. Furthermore, effects that are dominant today may be comparatively easy to eliminate: mechanism 1 of our Sec. 1 can be removed by using single-mode (i.e. thin) fibers, mechanism 2 by using monochromatic light. These techniques will not affect mechanism 3, which might therefore take on increeasing importance.

I should like to thank Drs. E. J. Friebele, G. H. Sigel, H. F. Taylor, and K. L. Bedford for helpful discussions of various aspects of this problem.

FOOTNOTES

1. This effect is often termed "mode dispersion"; e.g. ref. 4, Section 5.8.
2. Effect 2a) is usually called "material dispersion," and effect 2b) "waveguide dispersion"; see ref. 3.
3. Gloge, Marcatili, Marcuse, and Personick, "Dispersion Properties of Fibers" (Ch. 4 in "Optical Fiber Telecommunications," S. E. Miller and A. G. Chynoweth, eds., Academic Press, NY 1979).
4. J. E. Midwinter, "Optical Fibers for Transmission," (Wiley, New York, 1979).
5. One standard reference work actually uses this effect as its prime definition of the term "dispersion". International Dictionary of Applied Mathematics, (Van Nostrand, Princeton, 1960).
6. A brief qualitative mention of the effect appears in ref. 4, page 75.
7. J. W. Fleming, J. Am. Ceramic Soc. 59, 503 (1976), Fig. 1.
8. J. W. Fleming, personal communication.
9. Handbook of Optics, W. G. Driscoll, editor (New York, McGraw-Hill 1978) page 7-108.

FIGURE CAPTION

Figure 1. Fourier transforms $g(\nu)$ of signals $f(t) = e^{2\pi i \nu t} P(t)$ for different pulse shapes $P(t)$. All $P(t)$ are symmetric about the origin; for positive t, they are explicitly as follows.

Square $P(t) = \begin{cases} 1/2\tau & 0 < t < \tau \\ 0 & \tau < t \end{cases}$

Triangular $P(t) = \begin{cases} (\tau - t)/\tau^2 & 0 < t < \tau \\ 0 & \tau < t \end{cases}$

Quadratic $P(t) = \begin{cases} -(t^2 - \frac{3}{4}\tau^2)/\tau^3 & 0 < t < \tau/2 \\ (\frac{3}{2}\tau - t)^2/2\tau^3 & \tau/2 < t < 3\tau/2 \\ 0 & 3\tau/2 < t \end{cases}$

Gaussian $P(t) = e^{-(t/\tau)^2}/\tau\sqrt{\pi}$

P(t)	$g(\nu)$ with $u = \pi\tau(\nu-\nu_0)$
 square	$\sin 2u / 2u$
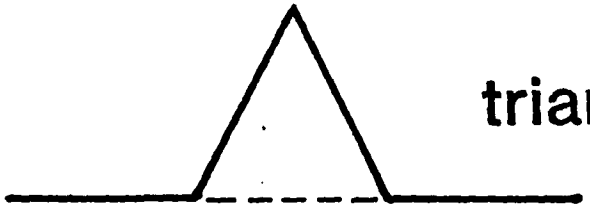 triangular	$(\sin u / u)^2$
 quadratic	$(\sin u / u)^3$
 gaussian	$\exp(-u^2)$

END

FILMED

10-83

DTIC